Limnol. Oceanogr., 53(5), 2008, 1816–1834

Thin layers of *Pseudo-nitzschia* spp. and the fate of *Dinophysis acuminata* during an upwelling–downwelling cycle in a Galician Ría

L. Velo-Suárez and S. González-Gil
Instituto Español de Oceanografía, Centro Oceanográfico de Vigo, Subida a Radiofaro 50-52, Cabo Estay, Canido, 36390 Vigo, Spain

P. Gentien and M. Lunven
Institut français de recherche pour l′explotation de la mer (IFREMER), Centre de Brest, Département dynamiques de l′environnement côtier, Pointe du Diable BP70, 29280 Plouzane, France

C. Bechemin
IFREMER/Laboratoire environnement ressources de pertuis charentais, Place du séminaire, L'Houmeau, France

L. Fernand
Centre for Environment Fisheries and Aquaculture Science (CEFAS), Pakefield Road, Lowestoft, Suffolk, NR33 OHT, United Kingdom (UK)

R. Raine
The Martin Ryan Institute, National University of Ireland, Galway, Ireland

B. Reguera
Instituto Español de Oceanografía, Centro Oceanográfico de Vigo, Subida a Radiofaro 50-52, Cabo Estay, Canido, 36390 Vigo, Spain

Abstract

Fine-resolution measurements of phytoplankton and physical parameters were made from 31 May to 14 June 2005 in the Ría de Pontevedra (Spain), which is subject to seasonal upwelling. The main objective of this work was to elucidate physical–biological interactions leading to subsurface aggregations of toxin-producing microalgae (*Pseudo-nitzschia* spp. and *Dinophysis* spp.). A sequence of upwelling-relaxation-upwelling-downwelling events was recorded with a moored Acoustic Doppler Current Profiler (ADCP). Thin layers (TLs) of *Pseudo-nitzschia* spp. and other diatoms (up to 30 μg chlorophyll *a* L^{-1}) developed and persisted in the pycnocline above cooler (12.5°C) upwelled water but were vertically displaced and even dispersed during downwelling. The establishment of steep pycnoclines after upwelling pulses and the formation of TLs of *Pseudo-nitzschia* spp. and other diatoms suggest that pycnoclines may act as retention areas for these populations. Their vertical displacement during downwelling would explain different patterns observed in the contamination of benthic resources and raft-mussels. A decimeter-scale segregation of *Pseudo-nitzschia micans* and *Dinophysis acuminata* populations was observed. The population of *D. acuminata*, present since March 2005 in Ría de Pontevedra, was never found within the pycnocline, did not perform any significant vertical migration, and was not dispersed during upwelling. Instead, it formed patches (up to 8×10^3 cell L^{-1}) in the warmer (15–18°C) surface (0–4 m) waters associated with a diurnal thermocline, and it spread throughout the ría into a near-surface layer during relaxation and downwelling. These results demonstrate the importance of considering species-specific behavior to predict the location of cell maxima.

Acknowledgments

We thank the crew of R/V *Mytilus* for their helpful attitude during the cruise, the Galician Monitoring Program (INTECMAR) for weekly reports on phytoplankton distributions in the Galician rías, and M.M. Daniélou and I. Ramilo for technical assistance. We acknowledge the constructive criticism of two anonymous reviewers.

This work was funded by the project "Harmful Algal Blooms Species in Thin Layers" (HABIT) from the 6th Framework Program of the European Commission (HABIT/GOCE-CT-2005-003932). This is a contribution to the Scientific Committee on Oceanic Research (SCOR) and Intergovernmental Oceanographic Commission (IOC) program on "Global Ecology and Oceanography of Harmful Algal Blooms (GEOHAB)," Core Research Project on "HABs and Stratification."

Chronic occurrences of toxin-producing *Pseudo-nitzschia* spp. and *Dinophysis* spp. cause the accumulation of Amnesic Shellfish Poisoning (ASP) and Diarrhetic Shellfish Poisoning (DSP) toxins, respectively, in shellfish above regulatory levels. These harmful algal events, which are not necessarily accompanied by high biomass of the toxic species, constitute the main threat for the shellfish industry in Europe. In the Galician Rías Baixas (NW Spain), ASP outbreaks caused by *Pseudo-nitzschia australis* (Míguez et al. 1996), coinciding with or followed by DSP outbreaks caused by *Dinophysis acuminata* (Reguera et al. 2003), are frequent events associated with thermohaline stratification during the early upwelling season (March–June). In order

to develop coupled physical–biological models for species of interest, it is necessary to have a sound knowledge of the species fine-scale distributions and behavior under a range of environmental conditions.

Thin layers (TLs) are structures that exhibit physical, chemical, and/or biological signatures that are different from the water just above and below. Their thickness ranges from a few centimeters to a few meters and can extend horizontally for kilometers and persist for days; planktonic organisms in these layers are substantially more abundant than in the water immediately above or below (Rines et al. 2002; McManus et al. 2003). Thin layers are usually associated with the main subsurface chlorophyll maximum, but several TLs may occur throughout the water column (Dekshenieks et al. 2001). Both physical (vertical shear, gradients in turbulence) and biological (swimming and buoyancy control; growth and mortality; physiological adaptations) processes are involved in the formation, maintenance, and dissipation of these structures (Donaghay and Osborn 1997; Genin et al. 2005; McManus et al. 2005). In the case of species that occur in low numbers, such as most *Dinophysis* spp., aggregation in TLs or in low-turbulence environments could represent a reproductive strategy by increasing probabilities of mating success, which might play a critical role in the life cycle of such species (Gentien et al. 2005).

Dekshenieks et al. (2001) provided specific criteria to classify an optical structure as a TL on the basis of the relative concentration of the organisms in the layer and its thickness. A thin layer, they argued, must be less than 5 m thick; must be coherent, i.e., the feature must be present in two or more subsequent profiles obtained with the high-resolution profiler; and must have an optical signal more than three times higher than the background signal. In this operational definition, the thickness of the layer was chosen to be less than 5 m because this is finer than the scale commonly sampled with oceanographic bottles and nets.

Traditional vertical sampling methods tend to either miss or underestimate local phytoplankton maxima because physical parameters and phytoplankton are not sampled at the same vertical resolution. However, advances in optical and acoustic instrumentation now allow high-resolution observations of the distribution of plankton organisms and their physical environment (Holliday et al. 2003). Several pennate diatoms and dinoflagellates, including toxic *Pseudo-nitzschia* and *Dinophysis* spp., have been reported to form TLs. *Pseudo-nitzschia australis*, *Pseudo-nitzschia pseudodelicatissima*, *Pseudo-nitzschia fraudulenta*, and *Pseudo-nitzschia pungens* have been observed in TLs in the San Juan Islands (Washington, USA) (Rines et al. 2002) and in Monterey Bay (Ryan et al. 2005; Sullivan et al. 2005). *Dinophysis acuminata*, *Dinophysis acuta*, and *Dinophysis norvegica* have been found to exhibit very heterogeneous vertical distributions in the Baltic Sea (Carpenter et al. 1995; Kononen et al. 2003, Setälä et al. 2005), Swedish fjords (Lindahl et al. 2007), the Galician rías (Reguera et al. 1995, 2003), and Thermaikos Bay (Koukaras and Nikolaidis 2004), and TLs of *D. acuminata* and *D. acuta* have been reported in the Bay of Biscay (Gentien et al. 1995) and in northern Portugal (Moita et al. 2006), respectively. Evidence has been presented on the diel vertical migration (DVM) of *D. acuminata* in the Galician Rías Baixas (Villarino et al. 1995), but in most cases, studies on vertical distributions of *Dinophysis* spp. have not been not accompanied by physical measurements with the appropriate spatial-temporal resolution (Maestrini 1998).

Maximum cell concentrations of different species of *Dinophysis* spp. have often been related to marked temperature- and salinity-driven density gradients in the water column (Maestrini 1998, and references therein; Koukaras and Nikolaidis 2004; Moita et al. 2006), but the key problem is determination of the cause of the increased numbers; are they due to in situ division rate (μ), physical accumulation, or a combination of both?

During spring 2005, a 2-week multidisciplinary cruise was conducted in Ría de Pontevedra (Rías Baixas, NW Spain) using advanced instrumentation designed for high-resolution sampling of the water column. The main objective of this work was to explore if *Pseudo-nitzschia* spp. and *Dinophysis* spp. formed TLs in the Ría de Pontevedra, and if so, how these layers responded to physical forcing during the upwelling season. A thin layer, in this work, is defined as a coherent and conspicuous heterogeneity (peak) in the vertical distribution of one or several species unequivocally identified with high-resolution profilers.

Material and methods

Study area—The Ría de Pontevedra (Fig. 1) was selected as the best location for studies related to *Pseudo-nitzschia* spp. and *Dinophysis* spp. based on historical monitoring records of cell abundance and shellfish harvesting closures (Blanco et al. 1998). Studies were carried out onboard R/V *Mytilus* from 31 May to 14 June 2005. Ría de Pontevedra, the second largest ría of the Galician Rías Baixas (NW Spain), has a surface area of 141 km^2, a mean depth of 31 m, and a volume of 3.5 km^3. This V-shaped ría widens progressively from Tambo islet in the innermost part toward the mouth, where it is connected to the coastal shelf by two entrances. The southern entrance is rather broad (7 km) and deep (60 m), and it provides the main channel for water exchange, whereas the northern entrance is narrower (3.7 km) and shallower (14 m). Two small islets, Ons and Onza, act as protective barriers against the swell of the open sea.

The hydrodynamics of the Ría de Pontevedra are driven mainly by freshwater runoff, water masses on the adjacent shelf, and the wind regime (Prego et al. 2001). Tidal forcing appears to be a minor factor since wind speeds higher than 4 m s^{-1} reverse surface currents against the tide. However, tides can be important locally in the innermost part of the Ría (Prego et al. 2001). The Lérez River (57 km) provides the main freshwater input; its monthly discharge rate ranges from 2 to 80 m^3 s^{-1} and closely follows rainfall patterns (De Castro et al. 2000).

Northerly winds promote seasonal upwelling of oceanic waters into the Galician Rías from April to October. Upwelling forces a two-layer, density-induced positive circulation in the ría, characterized by the outflow of

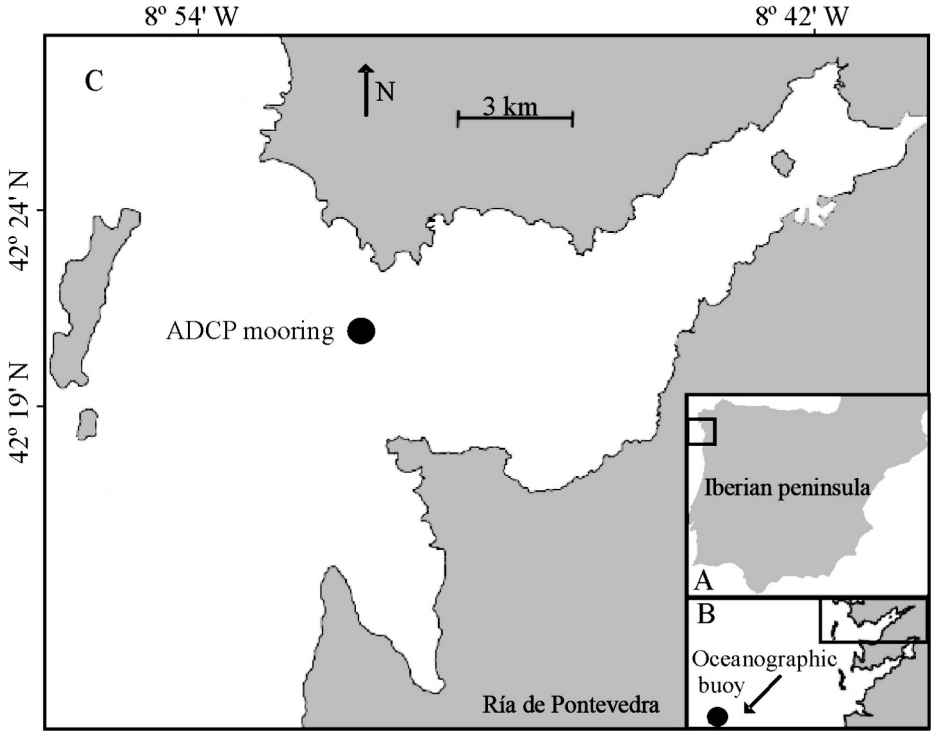

Fig. 1. (A) The Galician Rías Baixas (NW Iberian Peninsula). (B) The Ría de Pontevedra in relation to the Rías Baixas and the location of the Seawatch buoy of Puertos del Estado (www.puertos.es) off Cabo Silleiro. (C) Map of the study area showing location of the ADCP mooring (sta. 2).

surface water and the compensating inflow of upwelled water at the bottom (Álvarez-Salgado et al. 1993; Álvarez et al. 2003). Conversely, southerly winds that prevail in winter force surface coastal waters into the Rías Baixas, and downwelling fronts develop when they meet with inner waters influenced by freshwater runoff. Thus, during downwelling pulses, seaward outflow takes place in the bottom layer within the outer circulation cell, while the inner cell maintains a seaward circulation forced by runoff (Prego et al. 2001). Within each ría, wind-induced circulation patterns are highly influenced by local orographic effects at their entrance (De Castro et al. 2000).

Information on phytoplankton concentrations and environmental data for the area was obtained from weekly reports of the Galician Monitoring Centre (INTECMAR, www.intecmar.org).

Meteorology and hydrology—Locations where current measurements and meteorological data were collected are shown in Fig. 1. Wind and rainfall data were obtained from the Spanish Institute of Meteorology (INM, www.inm.es). Hourly mean values of wind speed and direction were estimated from data collected at the Cabo Silleiro buoy (Seawatch, Oceanor) (Fig. 1) (42°7.8′N, 9°23.4′W), which is part of an offshore network; its measurements are not biased by local features. Monthly averaged rainfall data were acquired from Peinador meteorological station (42°13.8′N, 8°37.2′W). Current velocity profiles were measured with a bottom-mounted Acoustic Doppler Current Profiler (ADCP) (RD Instruments, 614.4 kHz) moored at sta. 2, 45-m deep in the navigation channel (42°21.38′N, 8°50.07′W) in the outer part of the ría (Fig. 1). Reported current velocities are based on 2-min averages (bin size: 1 m) from raw ADCP data processed using the WinADCP software (RD Instruments). Scripts from the FATHOM Matlab toolbox for Multivariate Ecological and Oceanographic Data Analysis were used for vector manipulation and plotting.

Nutrients—An autoanalyzer (SAN System Plus, Skalar) was used for colorimetric determination of total ammonia nitrogen (TAN; $NH_4 + NH_3^+$) (Grasshoff et al. 1983, adapted to seawater) and NO_2^- (Bendschneider and Robinson 1952). NO_3^- was determined by cadmium–copper reduction to NO_2^- (Wood et al. 1967); PO_4^{++} and silicate concentrations were determined following Grasshoff et al. (1983). Silicate samples were kept refrigerated and in the dark until analysis to prevent silicon polymerization during storage. Nutrient analysis protocols are subject to regular intercalibration exercises within the Institut français de recherche pour l′explotation de la mer (IFREMER) laboratories.

The IFREMER particle-size analyzer profiler (IPSAP)—Measurements in the water column were carried out with the high-resolution IFREMER particle-size analyzer profiler (IPSAP), which includes a SBE25 conductivity-temperature-depth (CTD) probe (Sea-Bird Electronics), a

fluorescence sensor (Seapoint Sensors), and a particle-size analyzer (CILAS). The IPSAP profiler provides a synchronized set of data in real time, which is used for sampling guidance.

Based on diffraction pattern analysis, the particle-size analyzer (PSA) measures the total volume of particles present in an 8-mL free-flow cell and their size distribution over 30 size classes from 0.7 to 400 μm equivalent spherical diameter (Gentien et al. 1995). This method enables the quantification of phytoplankton populations, organic and inorganic particles, and organic matter aggregates. The PSA is connected to the SBE25 probe to allow real-time data acquisition of standard parameters, such as depth, temperature, salinity, chlorophyll-like in vivo fluorescence, and photosynthetically active radiation (PAR). The CTD fluorometer was calibrated with laboratory cultures of the diatom *Chaetoceros gracile* using the trichromatic method for chlorophyll determination according to Aminot and Kerouel (2004).

The profiler was equipped with a homemade video system, developed by Lunven et al. (2003), that allows in situ observation and quantification of suspended particles, which are collected and isolated in a capture-stilling chamber. This system was used to detect chain-forming diatoms (e.g., *Pseudo-nitzschia*) aggregated in thin layers.

At each station, the IPSAP profiler was lowered at a speed of 0.3 m s^{-1}, allowing an accurate assessment of the hydrological characteristics of the water column and the detection of water layers with distinct characteristics. During the up-cast, finer-scale measurements were carried out within these layers, and the instrument was stopped to collect samples from depths where structures of interest (fluorescence and particle-load maxima, pycnocline, and other density discontinuities) were detected. A 40-mm-diameter hose was attached to the profiler, close to the sensors, to allow an accurate sampling of specific layers. The use of a peristaltic pump, with a flow rate of 30 L min^{-1}, through a wide-bore pipe ensured minimum damage to delicate organisms. Microscopic observations onboard showed that this sampling method, which allows collection of living cells from their precise in situ locations, does not injure cellular structures.

The IFREMER Fine-Scale Sampler—The IFREMER Fine-Scale Sampler (FSS) (Lunven et al. 2005) was deployed to study the fine-scale vertical distribution of plankton species in relation to physical properties. This system consists of a ladder-like structure on which 15 2-liter oceanographic bottles were mounted horizontally, 20 cm apart between the central axes of two consecutive bottles. A SBE19 plus CTD probe (Sea-Bird Electronics) with a fluorescence sensor (Seapoint Sensors) integrated into the system allow optimal positioning in the water column.

The FSS was gently lowered to the target depth, chosen from the IPSAP profile readings, and towed horizontally for a few meters so that undisturbed water was sampled. Its design, featuring a large fin, slow forward speed (0.5 knot = 0.93 km h^{-1}), and smooth flow inside the bottles, produced minimal disturbance of the water layers. The 15 bottles were closed simultaneously by means of an electromagnetic trigger. On retrieval of the FSS, the water from each bottle was well mixed, and subsamples for phytoplankton counts and other analyses were collected.

During the survey, the FSS was deployed twice at sta. 3 (Fig. 2) in the Ría to describe the fine decimeter-scale distribution of *Dinophysis* and accompanying species. Water samples were examined as described in the following section.

Phytoplankton sampling—Sampling locations for nutrients and phytoplankton are shown in Fig. 2. To obtain qualitative information on phytoplankton distribution, vertical hauls with plankton nets (20-μm mesh) and size-fractioned (20–70 μm) live samples, concentrated through a set of superimposed screens with different mesh sizes, were collected with the peristaltic pump at selected depths and immediately examined onboard under a ZEISS Axiovert microscope at $\times$100 and $\times$400 magnification. For quantitative information, two kinds of samples were collected from discrete depths with the peristaltic pump: (1) unconcentrated seawater samples, to analyze the whole phytoplankton community, and (2) 1-liter seawater samples concentrated through 20-μm filters to a final volume of 50 mL. Different kinds of preservatives—Lugol's iodine acidic solution, buffered formaldehyde (4%), and glutaraldehyde (1%), each suitable for the different microscopy techniques used—were used in subsamples of each sample.

Lugol-fixed samples were analyzed under an inverted microscope (Nikon Eclipse 2000) using the method described in Utermöhl (1931). The volume of the sedimentation chambers (10–25 mL) was chosen after reading the chlorophyll–fluorescence profiles at each station. If chlorophyll *a* (Chl *a*) values were higher than 15 μg L^{-1}, sedimentation columns of 10 mL were used to prevent the overlay of phytoplankton cells at the bottom of the chamber. Phytoplankton abundance was determined to species level when possible. Two transects were counted at $\times$400 magnification to include the smaller and more abundant species. To count larger, less abundant species (including *Dinophysis* spp.), 3-mL aliquots of the concentrated samples (factor: 1 : 20) were placed in sedimentation chambers, and the whole surface of the chamber was scanned at a magnification of $\times$100, so that the detection limit was 17 cell L^{-1}.

For the ultrastructural examination of diatom frustules, selected glutaraldehyde-preserved samples were treated with acid (70% nitric acid; Boyle et al. 1984) and examined under a Hitachi 700 transmission electron microscope (Hitachi Instruments).

Results

Meteorological and hydrographical conditions during the survey—Northerly winds (which favor upwelling) were predominant during the cruise, although there was a shift to southerly winds on 09 June. Northerly winds were strongest (Fig. 3) at the beginning of the cruise, with a mean velocity of 7.7 m s^{-1} and a maximum of 11.7 m s^{-1} over the period 31 May to 08 June. Toward the end of the cruise, winds became southerly, with a mean velocity of 3.07 m s^{-1} and a maximum of 7 m s^{-1} from 09 to 13 June.

Coupled to the northerly wind, hourly records indicated a daily sea–land breeze cycle between 31 May and 02 June,

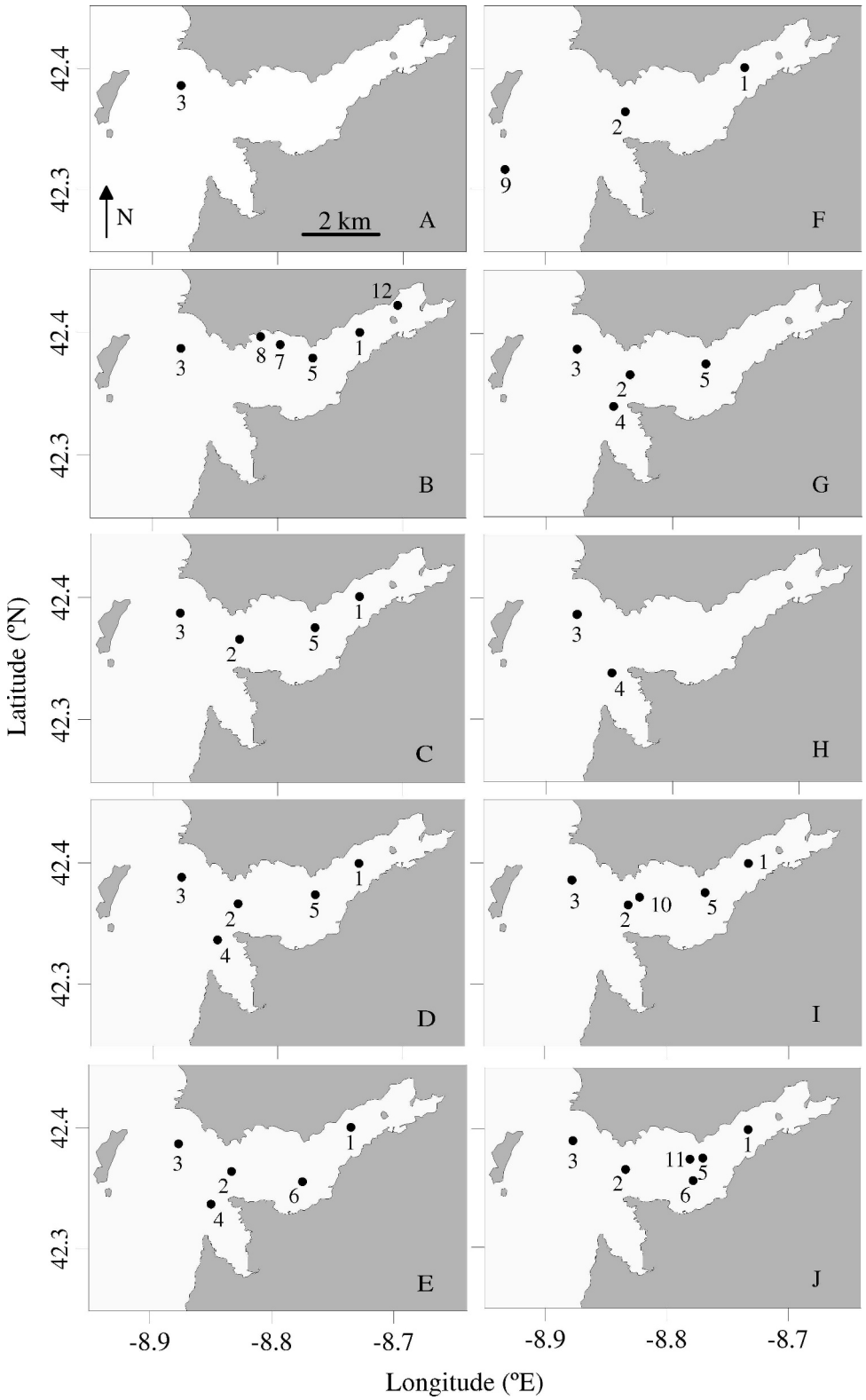

Fig. 2. Spatial and temporal distribution of IPSAP profiler sampling sites in the Ría de Pontevedra during the survey. (A) 31 May, (B) 01 June, (C) 02 June, (D) 03 June, (E) 06 June, (F) 07 June, (G) 08 June, (H) 09 June, (I) 10 June, and (J) 13 June. All dates are 2005.

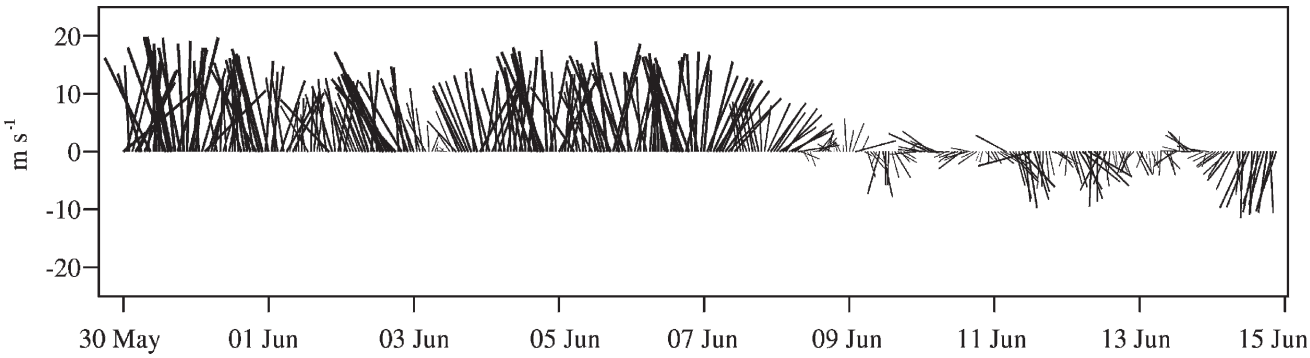

Fig. 3. Hourly measurements of wind direction and velocity (m s^{-1}) recorded at the Seawatch buoy in Cabo Silleiro.

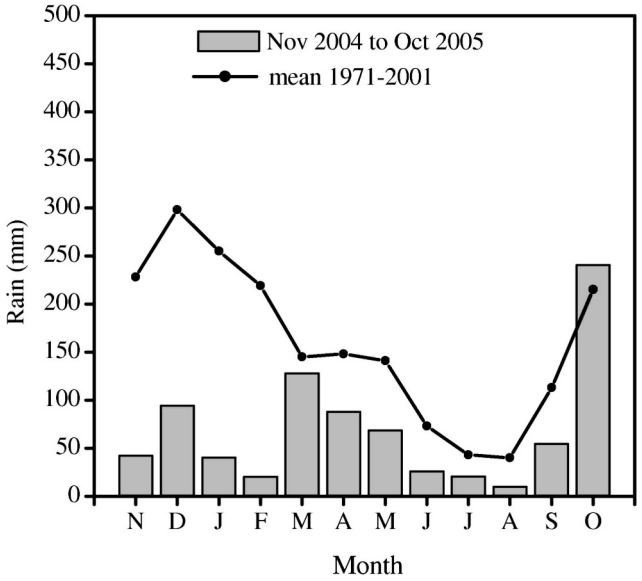

Fig. 4. Monthly rainfall (2004–2005) and the 31-yr (1971–2001) monthly mean in Pontevedra (Peinador national meteorological station; www.inm.es).

resulting in northwesterly (inshore) winds during daytime and northeasterly (offshore) winds during the evening and night. This pattern occurred at the beginning of the cruise due to stable atmospheric conditions and warm air temperatures (up to 25°C).

Figure 4 shows monthly rainfall from November 2004 to October 2005 and the 31-yr (1971–2001) mean monthly rainfall. In 2005, winter rainfall (January–March) was 30% below the long-term mean. Spring (April–May) rainfall was still 50% below average but followed the long-term trend.

Changes in seawater temperature and salinity at sta. 2 are shown in Fig. 5. Upwelling, induced by northerly winds, persisted from the beginning of the cruise to 09 June, with a brief relaxation 02–03 June. CTD profiles (depth 40 m) showed water with the characteristics of the Eastern North Atlantic Central Water (ENACW; 35.67 < salinity < 35.83; 11.8°C < temperature < 13.5°C; Fiuza et al. 1998) in the ría at 5–10-m depth (07 June). After 09 June, downwelling occurred under weak southerly winds, followed by stronger southeasterly winds at the end of the survey. Seawater temperatures ranged from 18°C at the surface to 12°C near the bottom, but changes in salinity were extremely small (35.4–35.8). Thus, density gradients in the water column at this station were primarily due to differences in water temperature.

A vector plot from the bottom-mounted ADCP (Fig. 6) located in the center of the navigation channel (sta. 2) shows the main periods of inflow and outflow at all measured depths. Surface currents (0–4 m) were not reliably measured with the bottom-mounted ADCP. For the remainder of the water column, the following comments can be made. For the depths below 4 m, there was inflow at all depths from 31 May to 01 June. From 01 to 03 June, in response to relaxation of northwesterly winds, there was a period of outflow in the bottom layer and inflow above the thermocline. Two days later, when northwesterly winds increased, inflow again occurred throughout the water column until 09 June. At this time, there was a shift to southerly winds, with decreased (<3 m s^{-1}) intensity, so that a strong outflow was evident near the seafloor, and inflow occurred closer to the surface. The progressive vector plot (Fig. 7) illustrates this two-layer behavior and emphasizes the vertical shear of the residual flow. The vertical shear of horizontal velocity was generally low (<0.003 s^{-1}). Shear values up to 0.01 s^{-1} were recorded at the boundary between ENACW and subsurface waters during the cruise, and the maximum of 0.023 s^{-1} at 17 m occurred during the downwelling pulse at the end of the survey. Shear recorded in the 5–10-m depth range was generally higher than 0.025 s^{-1}.

Transects taken daily across the mouth of the ría with a ship-mounted ADCP (not shown) confirm that the mooring data were indicative of the water movements to the south of the ría during upwelling pulses. The main surface outflow during the upwelling period was observed in the northern part of the ría.

Nutrients and Chl a distributions—At 30 m, upwelled waters with the signature of ENACW contained high concentrations of inorganic nutrients (dissolved inorganic nitrogen, phosphates, and silicates; Fig. 8). Nutrient concentrations, especially silicates, were much lower in the Chl *a* maximum (7–10 m) and practically depleted in surface waters.

Discrete-depth water samples revealed an increase in phytoplankton biomass throughout the Ría between the

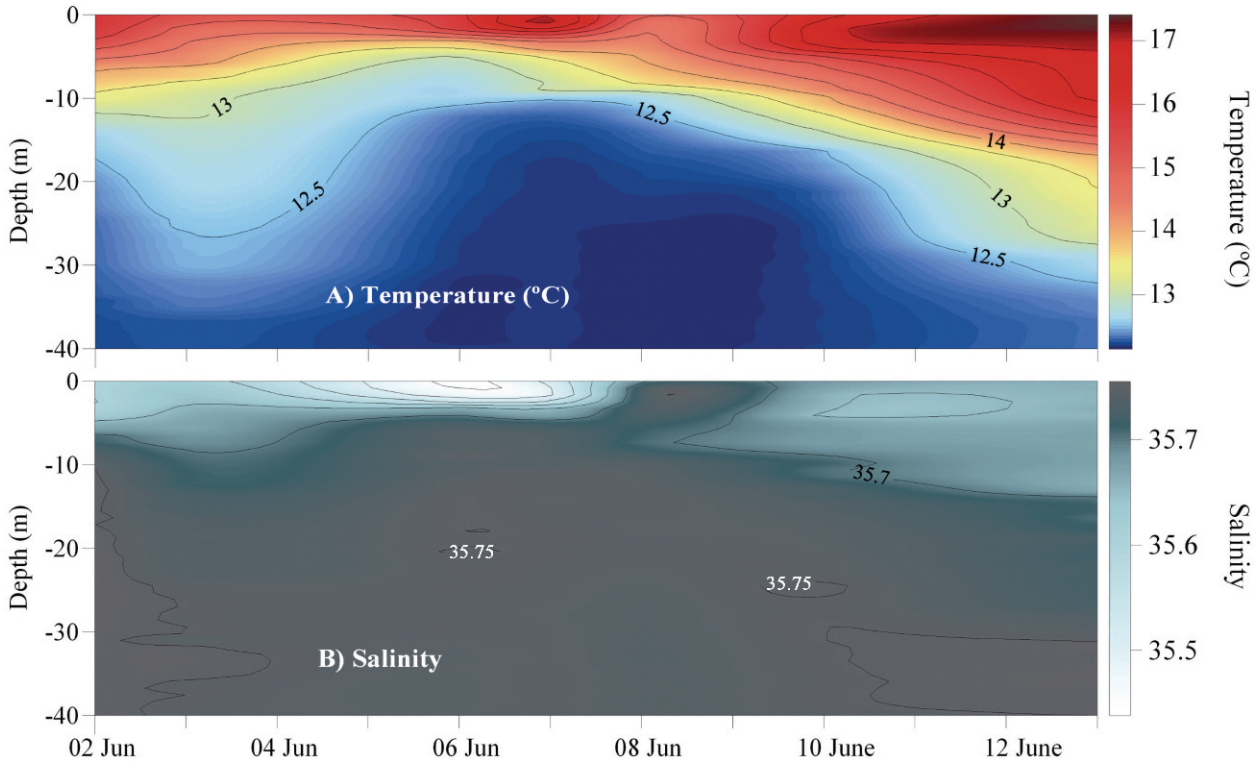

Fig. 5. Vertical distribution, from 02 to 13 June 2005, of (A) temperature (°C) and (B) salinity recorded at sta. 2 where the ADCP was moored.

26.9 and 27.1 σ_t (potential density) isopycnals, i.e., at the boundary between ENACW and the mixed surface–water masses. Chl *a* estimates up to 25 μg L^{-1} in the pycnocline (27.0 σ_t) were ~5 times higher than in the water above and below. The close relationship between the vertical gradient in σ_t and the Chl *a* maxima at different stations during the cruise (Fig. 9) suggests that a single, coherent TL was present throughout the area. The depth and thickness of the TL, which generally corresponded to the location of the 27 σ_t isopycnal, were spatially variable across the ría—thinner and shallower at the entrances to the Ría and less well defined at the innermost stations. This trend was most pronounced from 02 to 07 June, before the downwelling event (Fig. 3).

At sta. 3 (Fig. 10) (42°23.2′N, 8°52.6′W), the intrusion of upwelled ENACW waters on 31 May enhanced the TL formation and raised the location of the 27 σ_t isopycnal and Chl *a* maximum to 7–8-m depth. On 06 June, the TL was eroded due to upwelling relaxation caused by lower mean velocities of northerly winds. The IPSAP profile at sta. 3 on that day showed a homogeneous distribution of Chl *a* within the water column. A new upwelling pulse promoted the re-formation of the TL located above ENACW bottom waters. This TL developed and persisted within the 27 σ_t isopycnal until it was vertically displaced and eroded by downwelling waters at the end of the cruise (13 June).

The same pattern was also observed within sta. 2 (Fig. 11) (42°27.7′N, 8°50.01′W). The TL was always located between the 26.9 σ_t and 27.1 σ_t isopycnals, and it became narrower during the second upwelling pulse. However, it was eroded and mixed on 08 June in the navigation channel stations, while it could still be observed (close to the bottom) at sta. 3 until 12 June.

Light availability within the TL varied from <1% to almost 20% of the incident radiation during upwelling pulses. Lower light levels (~1–2%; 7.79 μmol photons m^{-2} s^{-1}) were found at the innermost stations, where TLs were not well defined and phytoplankton within these thicker layers caused self-shading. Conversely, higher light levels (~10–18%; 180 μmol photons m^{-2} s^{-1}) were found during the second upwelling pulse at the outermost stations where the TL was thinner and shallower. When the TL was displaced downward, light availability within it became progressively lower, until it was <1% of the incident light (3203 μmol photons m^{-2} s^{-1}) on 13 June.

Phytoplankton communities—Vertical net tows at each station and shipboard observations showed that diatoms were dominant throughout the water column at the beginning of the cruise (from 31 May to 09 June). The diatom community consisted of a mixture of medium- and large-sized species (e.g., *Chaetoceros curvisetus*, *Chaetoceros didymus*, *Leptocylindrus danicus*, *Guinardia delicatula*, and *Pseudo-nitzschia* spp.) as well as small *Chaetoceros* species (*Chaetoceros socialis*). Cell counts of preserved samples showed that *C. socialis* and *Pseudo-nitzschia* spp. (up to 1.5×10^6 cell L^{-1}) were the numerically dominant species within the TL; other diatoms (Fig. 12) showed lower cell abundances ($<5 \times 10^5$ cell L^{-1}). *Chaetoceros* spp. together with *Pseudo-nitzschia* spp. made up more

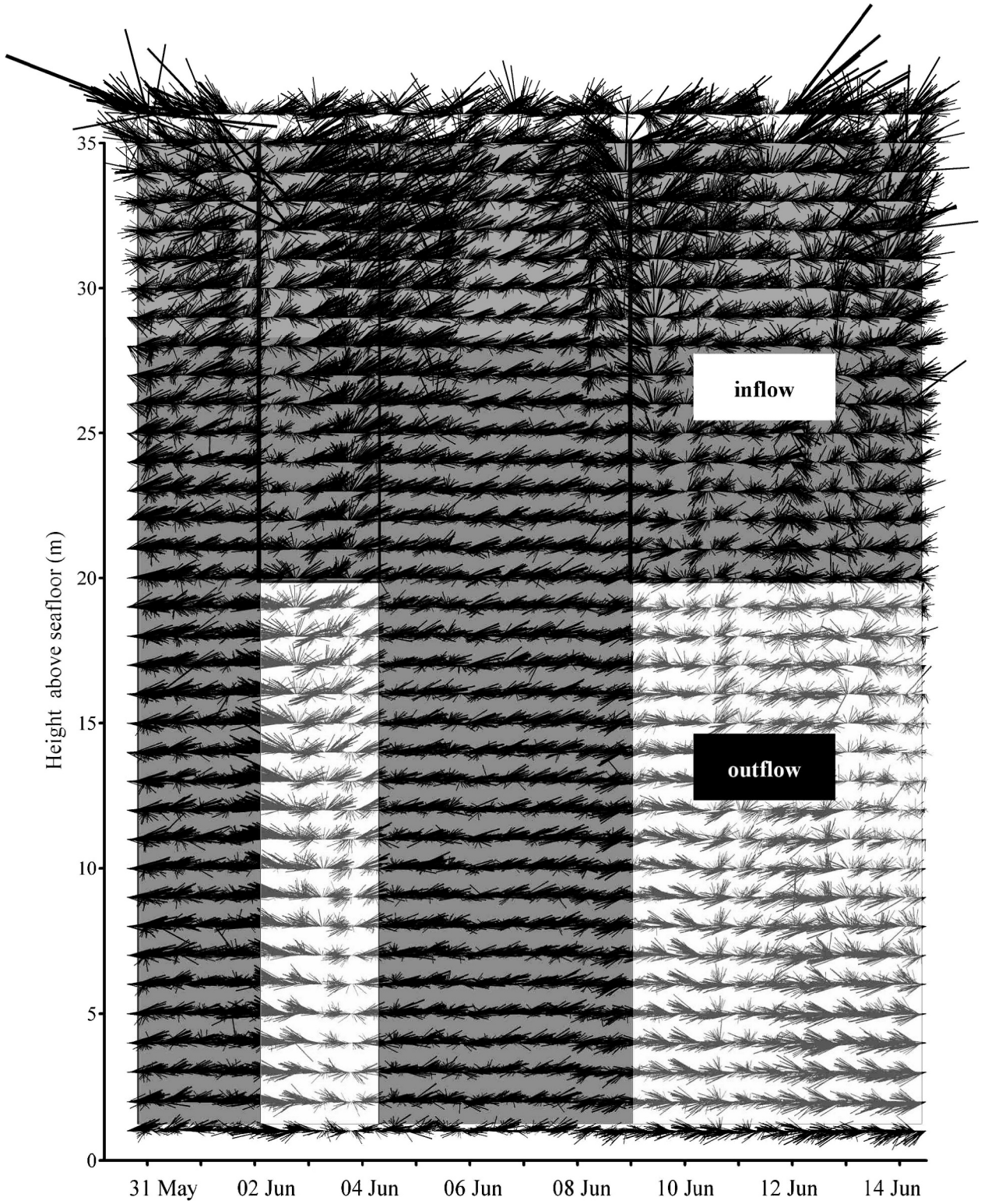

Fig. 6. Vector plot from the bottom-mounted ADCP showing the main periods of inflow (gray) and outflow (white) from 30 May to 14 June 2005.

than 70% of the diatom population at all depths in all sampled stations.

Two species of *Pseudo-nitzschia* were identified by electron microscopy: *Pseudo-nitzschia australis* (Fig. 13), a known domoic acid-producer in the Galician Rías (Míguez et al. 1996), which occurred in free chains within the water column, and *Pseudo-nitzschia* cf. *pseudodelicatissima* (Fig. 14), which occurred both in free chains and embedded

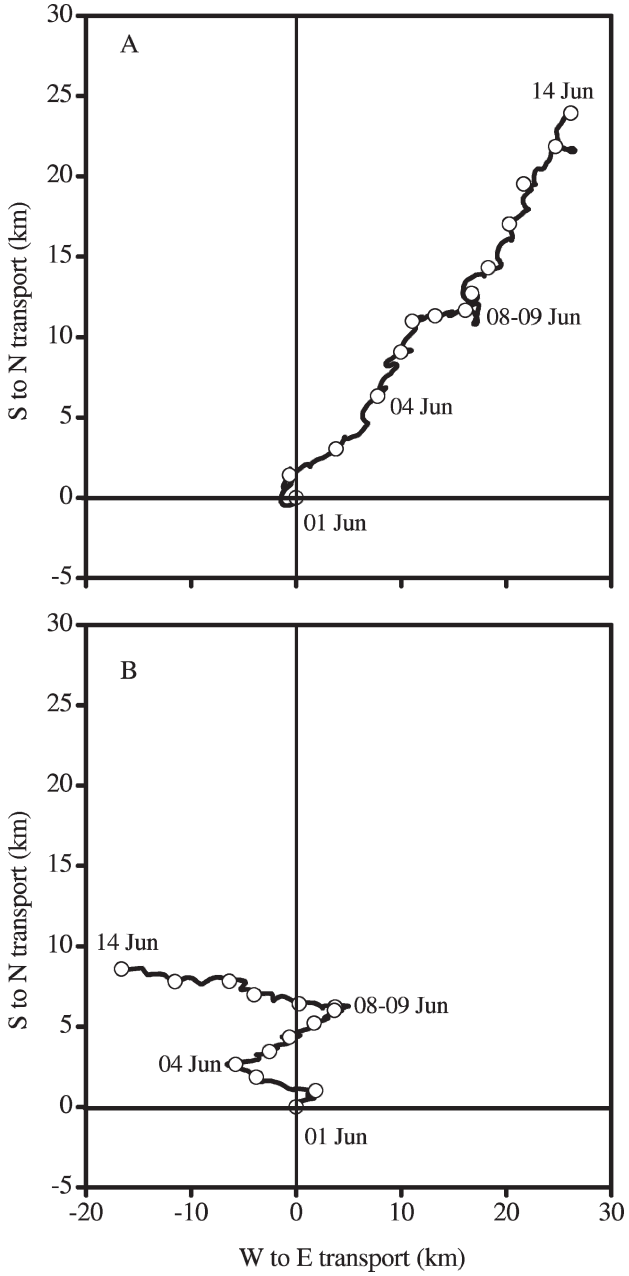

Fig. 7. Progressive vector diagrams (PVDs) of current data from the moored ADCP at 10 m (A, bin 31), and 40 m (B, bin 5) from 01 to 14 June. Data start at the origin (0,0). Dots are positioned at midnight (00:00 h). Note the divergence between upper and lower layers on 03 June and again on 10 June.

as single cells or pairs within spherical colonies of *C. socialis*. Although fixatives and storage caused the disruption of these colonies, it was possible to observe this association in live samples onboard.

By the end of the cruise, after upwelling-favorable winds had ceased (09 June), dinoflagellates became dominant, and diatoms were displaced downward. The previous TL could be detected close to the bottom at several stations, and the phytoplankton community from this layer was mainly composed of empty frustules and decaying (broken,

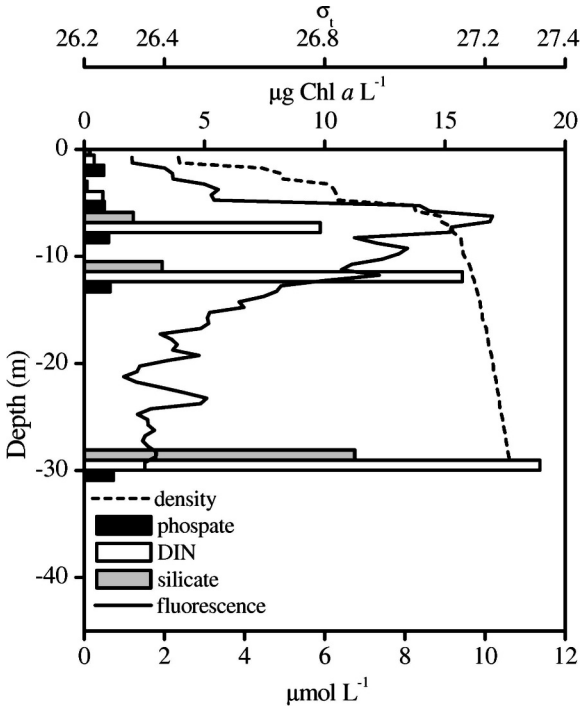

Fig. 8. Typical (upwelling-promoted) vertical distribution of phosphate, dissolved inorganic nitrogen (DIN), and silicates (μmol L^{-1}), seawater density (σ_t), and in vivo fluorescence (μg Chl *a* L^{-1}) during the second upwelling pulse (08 June, sta. 3) in Ría de Pontevedra.

infested with bacteria and ciliates) colonies of *C. socialis*, *Pseudo-nitzschia* spp., and other diatoms. At the surface, the phytoplankton community was dominated by *Prorocentrum micans*, *Ceratium* spp., *Protoperidinium* spp., *Gymnodinium* spp., and *D. acuminata*.

Distribution of D. acuminata—Table 1 and Fig. 15 show the distribution of *D. acuminata* abundance during the cruise. Patches of high cell abundance (5×10^3 cell L^{-1}) were found randomly throughout the ría but never associated with the 27 σ_t isopycnal (10 m), where diatoms were dominant, except at one profile in sta. 2 (07 June) (*see* Table 1). *Dinophysis acuminata* was almost always aggregated in the warmer (15×18°C) surface (0×6 m) waters, and the species maximum was associated with the diurnal thermocline. One isolated patch of 10^3 cells L^{-1} was found below the 27 σ_t isopycnal at 21-m depth in cold upwelled waters on 31 May (sta. 3). In this case, *D. acuminata* occurred within the ENACW nutrient-rich waters below the diatom TL at the pycnocline. From 31 May to 08 June, when the water column was highly stratified, high concentrations (>2.5×10^3 cell L^{-1}) of *D. acuminata* were found in some, but not all, sampled stations. The highest abundance (9×10^3 cell L^{-1}) occurred at 0–6-m depth, whereas concentrations within the pycnocline were always below 500 cell L^{-1}. Patches of the phototrophic ciliate *Myrionecta rubra* (= *Mesodinium rubrum*), recently described as an optimum prey for *D. acuminata* in culture (Park et al. 2006), were also found within the same depth range on 06–07 June at some profiles (data not shown).

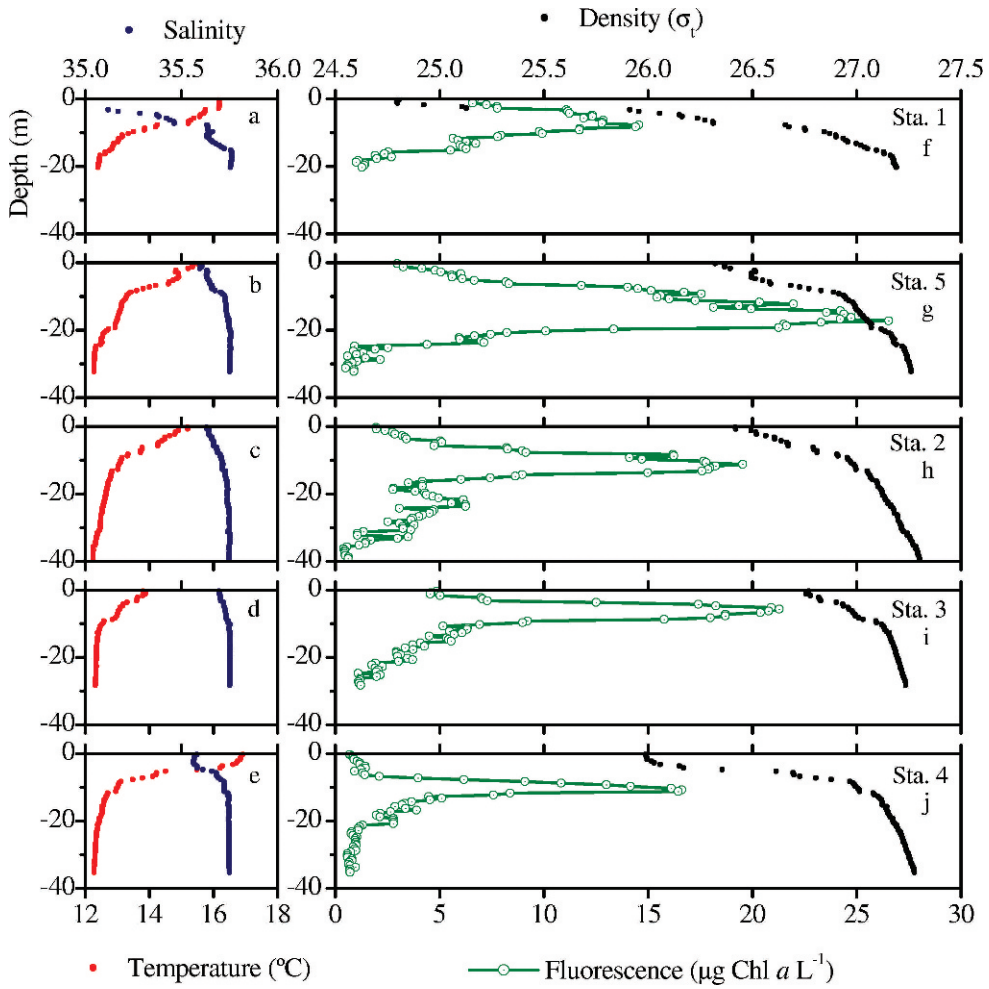

Fig. 9. Physical and optical structure in Ría de Pontevedra on 03 June 2005. (A–E) Temperature (red) and salinity (blue); (F–J) sigma theta (black) and Chl *a* concentration (green) profiles. *See* Fig. 2D for locations.

Myrionecta rubra was initially missed in live plankton concentrates because the ciliate cells easily burst when passed through meshes. Nevertheless, they were observed in the Lugol-fixed samples.

On 13 June, when downwelling conditions caused piling of warmer shelf waters into the *R*ía, and disruption of stratification, *D. acuminata* reached its highest concentration (9×10^3 cell L^{-1}) and spread throughout the whole ría. This species formed a continuous near-surface TL located in the warmer surface waters associated with the diurnal thermocline. Thus, *D. acuminata* was still most abundant in the surface layer and not associated with the diatom TL at the 27 σ_t isopycnal. Vertical distributions of cell concentrations over a 24-h cycle showed that *D. acuminata* was always restricted to the 0–5-m depth waters.

High-resolution (decimeter-scale) vertical distribution of Dinophysis *spp.*—On 09 June, the FSS was deployed across the depth ranges 0–3 and 8–11 m at sta. 3 (42°23.2′N, 8°52.6′W). Wind speeds were low (0.5 to 4 m s^{-1}), providing optimal conditions for fine-scale sampling. A previous IPSAP profile showed a pycnocline at around 10 m and a TL (15 µg Chl *a* L^{-1}) at the base of this pycnocline (Fig. 16A). Vertical distributions of *D. acuminata*, *P. micans*, and *Ceratium fusus* are shown in Fig. 16B and Fig. 16C. *Prorocentrum micans* concentrations showed two maxima with up to 4500 cell L^{-1} in the uppermost layer close to the surface (0.2 and 0.8 m), but abundance dropped to less than 100 cell L^{-1} below 2 m. *Dinophysis acuminata* concentration in the upper layer was always >1000 cell L^{-1}, and its highest abundance was observed between 1.5 and 2.0 m, just below the *P. micans* maxima. In contrast, *D. acuminata* and *P. micans* abundances in the 8–11 m layer were considerably lower (<100 cell L^{-1}), or below detection limits in the case of *P. micans*. *Ceratium fusus* was not detected in the upper layer, but its concentration increased to almost 3000 cell L^{-1} at 9 m, where it became the dominant dinoflagellate species. Other dinoflagellates, such as *Ceratium furca*, were also present in high numbers and co-occurred with diatoms at the TL located at the bottom of the pycnocline.

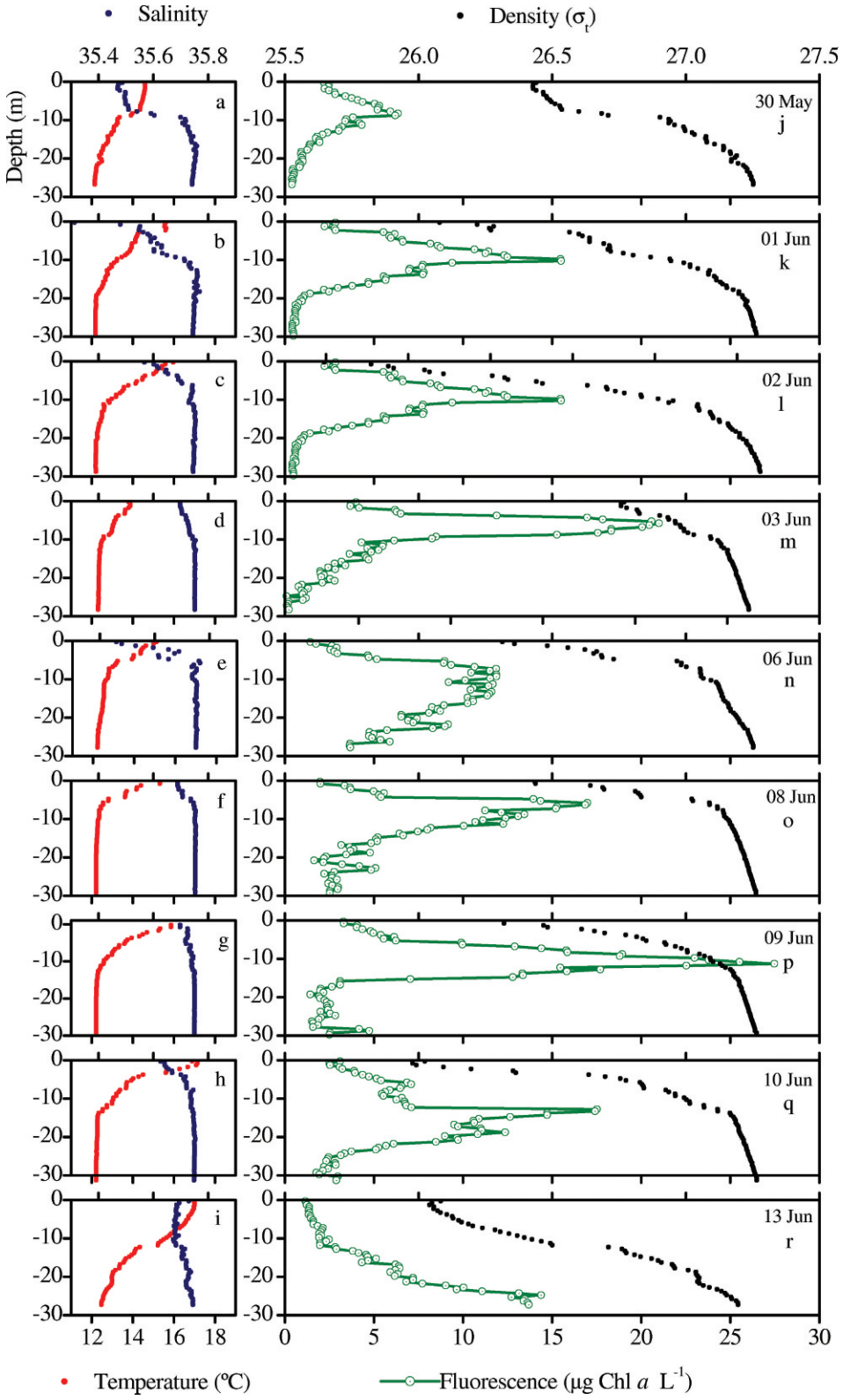

Fig. 10. Vertical distribution of (A–I) temperature (red) and salinity (blue); (J–R) sigma theta (black) and Chl *a* concentration (green) at sta. 3 (Ría de Pontevedra) from 30 May to 13 June.

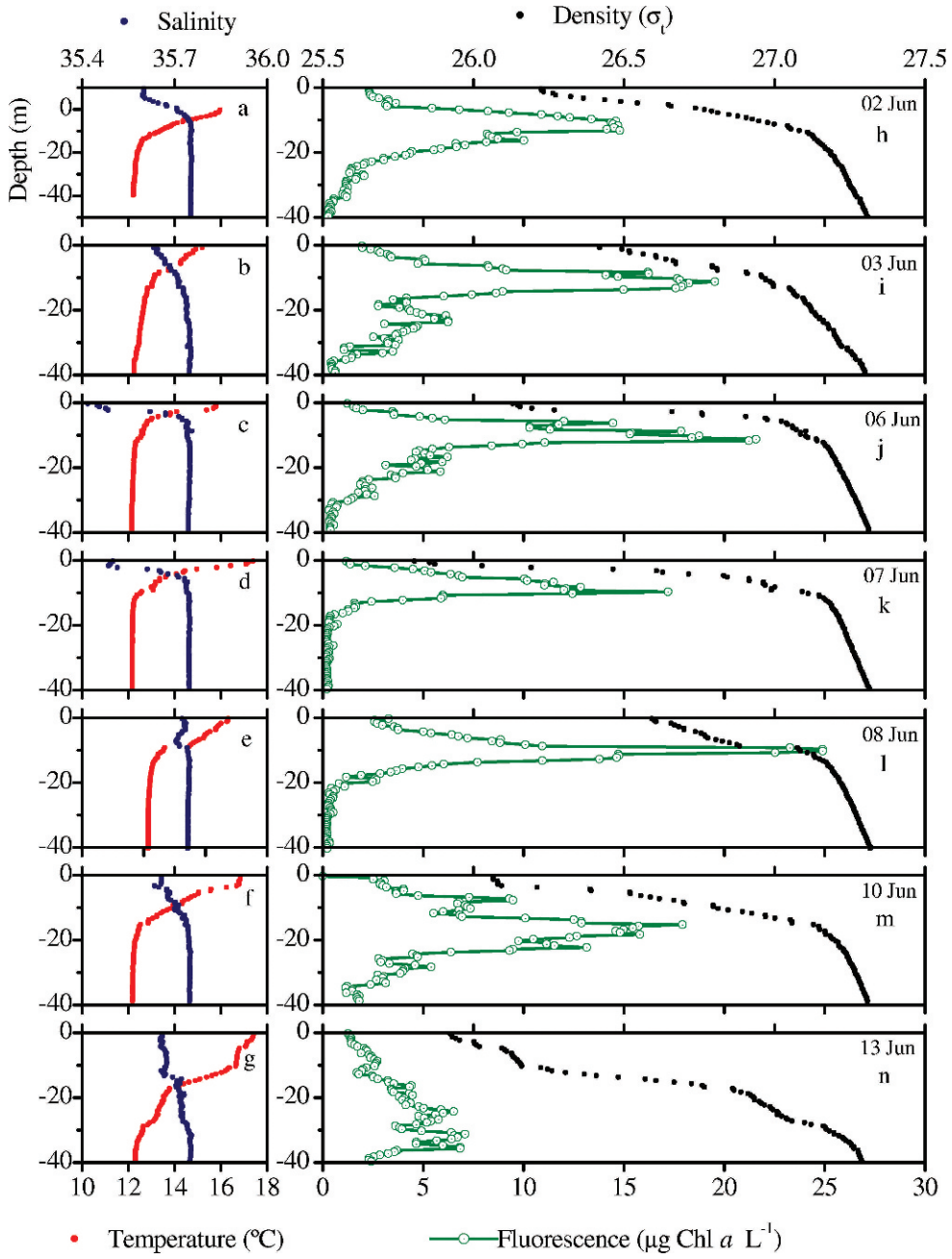

Fig. 11. Vertical distribution of (A–G) Temperature (red) and salinity (blue); (H–M) sigma theta (black) and Chl *a* concentration (green) at sta. 2 (Ría de Pontevedra) from 02 June to 13 June.

Discussion

Thin layers of Pseudo-nitzschia *spp. and other diatoms*—Our results show that northerly (upwelling-favorable) winds in Ría de Pontevedra promoted shoaling of the pycnocline and strengthening of density gradients in the water column following the introduction of cool, nutrient-rich ENACW waters into the ría. *Pseudo-nitzschia* spp. were closely associated with the pycnocline located at the boundary between the ENACW and the surface-water masses. The location of this layer at a depth that may represent a trade-off between sufficient light intensity and high nutrient concentrations would explain the diatom-abundance levels recorded. Unfortunately, it was not possible to calculate photosynthesis-irradiance (P-I) curves for *Pseudo-nitzschia* spp. because they were mixed with other diatom species during our survey. However, studies on *Pseudo-nitzschia* spp. in laboratory cultures (Bates 1998, and reference therein) have shown that *Pseudo-nitzschia* spp. can achieve high division rates at irradiance levels above 90 μmol photons m^{-2} s^{-1}, a value one half of some observed within the TL (180 μmol photons m^{-2} s^{-1}) at sta. 3 in Ría de Pontevedra.

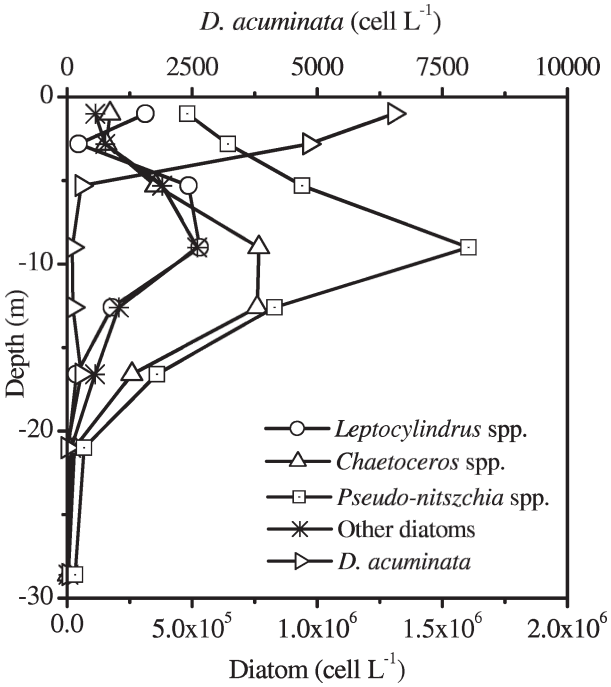

Fig. 12. Typical vertical distribution during the upwelling pulse (sta. 3; 02 June) of the diatom assemblage (bottom axis) showing that *Chaetoceros* spp., and *Pseudo-nitzschia* spp. were the dominant species. *Dinophysis acuminata* is shown in the top axis (note differences in absolute values).

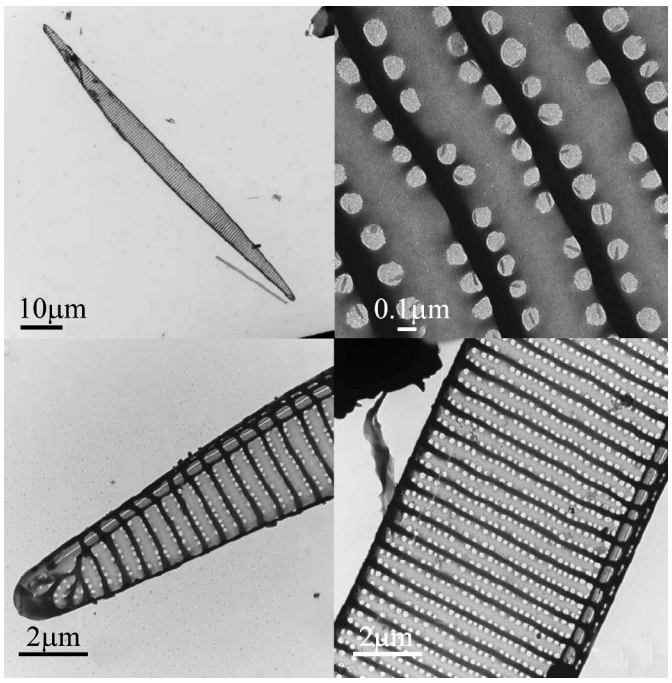

Fig. 13. Transmission electron microscopy (TEM) micrographs of *Pseudo-nitzschia australis*.

Passive accumulation of cells by sedimentation due to deceleration of sinking rate in the pycnocline (Gallager et al. 2004), together with the highest vertical shear observed in the water column, may also have contributed to form

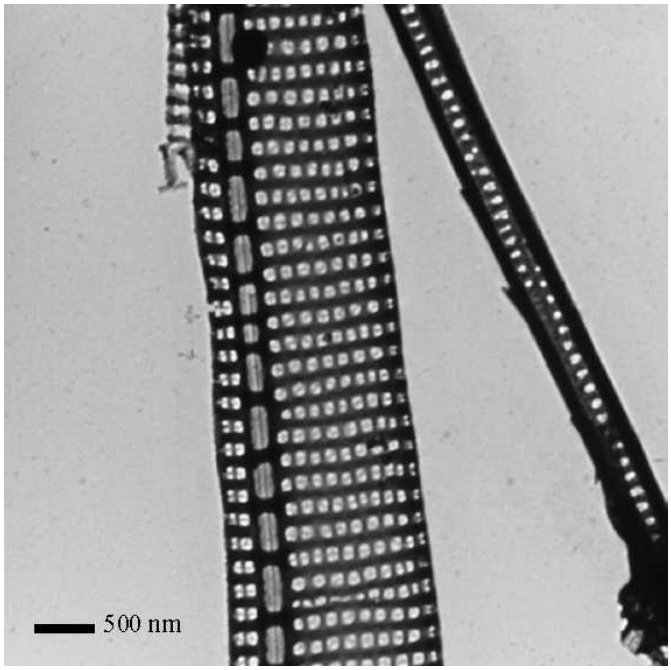

Fig. 14. Transmission electron microscopy (TEM) micrograph of *Pseudo-nitzschia* cf. *pseudodelicatissima*.

and maintain this layer. The Chl *a* concentrations detected on this cruise with the high-resolution profiler are exceptionally high for the Galician Rías. Previous studies with conventional sampling methods in Ría de Vigo reported maximum values of Chl *a* around 8 μg L^{-1} (Nogueira et al. 1997).

Klausmeier and Litchman (2001) simulated the formation of TLs by motile phytoplankton cells under stratified conditions. They found that TLs are optimally located at depths where phytoplankton would be equally limited by nutrients and light, where the concentration of limiting nutrients is low and constant above the TL and linearly increases with depth below it. Increased supplies of nutrients would make the TL move closer to the surface and increase its biomass. The thickness of the TL would be determined by the degree of turbulence, so that very thin layers would be observed in small and poorly mixed systems. During our cruise and following both upwelling pulses (Figs. 10, 11), the TL shoaled after the new addition of nutrients, giving a vertical structure in accordance with that of Klausmeier and Litchman's (2001) model (Fig. 8). Further, the TL was thinner at sta. 3, where a combination of nutrient supply, steep density gradients, and increased light levels occurred, and thicker in the innermost parts of the ría (sta. 1), which were more affected by tidal mixing.

The effect of turbulence dissipation on a TL of coccolithophores in well-stratified waters of the western English Channel was discussed by Sharples et al. (2001): turbulence enhanced phytoplankton growth by supplying nutrients from near-bottom waters but reduced phytoplankton concentration at the base of the TL by mixing its cells into bottom waters. In our study, the upper part of the TL was more defined than the lower part (Figs. 10, 11). Once downwelling events started, the TL was displaced

Table 1. Depths (in m) of *D. acuminata* cell maxima at each station during the survey.

Sta.	31 May	01 Jun	02 Jun	03 Jun	06 Jun	07 Jun	08 Jun	09 Jun	10 Jun	13 Jun
1	–	6	1.2	3.3	1.2	3.8	–	–	1.3	3
2	–	–	5.4	5.4	3.3	8.8	0.8	–	1.4	3.2
3	21	5	1.1	0.9	1.1	–	1	2	3	1
4	–	–	–	4.5	5.8	–	4.4	2	–	–
5	–	3	3.4	0.8	–	–	8.5	–	0.7	2.3
6	–	–	–	–	1.4	–	–	–	–	4.7
7	–	0.6	–	–	–	–	–	–	–	–
8	–	1	–	–	–	–	–	–	–	–
9	–	–	–	–	–	–	–	–	–	–
10	–	–	–	–	–	–	–	–	2.4	–
11	–	–	–	–	–	–	–	–	–	3
12	–	2	–	–	–	–	–	–	–	–

downward. Increased turbulence due to tidal forcing may have caused the TL erosion in the innermost parts of the ría, whereas in the deeper, outermost stations, less affected by tides, the TL could still be observed at the end of the cruise.

Stacey et al. (2007) discussed the effects of turbulent dissipation combined with three TL-convergence mechanisms: straining (vertical shear of the horizontal current), motility, and buoyancy. These authors concluded that layer thickness and maintenance in stratified systems were enhanced by reduction of turbulent diffusion. Whilst motility and buoyancy could maintain a TL indefinitely, straining processes tended to disperse already formed TLs by increasing turbulent diffusion.

The TL of *Pseudo-nitzschia* spp. located at the $\sigma_t = 27$ isopycnal in Ría de Pontevedra developed and persisted during upwelling and relaxation and was displaced toward the bottom during downwelling. Therefore, the near-bottom layer of *Pseudo-nitzschia* spp. found on 13 June resulted from physical displacement rather than sinking of a senescent population. This study clearly shows a coupling between physical processes (upwelling) leading to increased nutrient levels, strengthening of the pycnocline, and reduction in vertical mixing, and the biological development of dense TLs of *Pseudo-nitzschia* spp. and *C. socialis*, and the subsequent, displacement of this ''toxic mat'' to the bottom during downwelling in the Galician Rías Baixas. In a similar way, Rines et al. (2002) described near-surface TLs of *Pseudo-nitzschia* spp. located around the $\sigma_t = 29.8$ isopycnal in the San Juan Islands, U.S.A. In that study, near-bottom layers, still associated with the $\sigma_t = 29.8$ isopycnal, were found after a river plume covered the study area. In this study, TLs were displaced by downwelling pulses, whereas in that of Rines et al. (2002), the TL was displaced by a river plume. Although they are two different scenarios, in both cases, lower-density water masses caused the displacement of the TL and promoted similar results. Nevertheless, density gradients in the rías during this (2005) exceptionally dry spring, were driven by changes in temperature, whereas those in the San Juan Islands (Rines et al. 2002) were mainly driven by changes in salinity and were much more pronounced.

Aggregates of *C. socialis* colonies with *P. pseudodelicatissima* embedded in them have been reported before. Fryxell et al. (1997) described passively formed aggregates of the two species. In contrast, Rines et al. (2002) suggested that these two genera may actively live in close association with each other because *C. socialis* colonies provide a competitive advantage by offering a sheltered microenvironment to *Pseudo-nitzschia* spp. within the water column (Bates and Trainer 2006).

Thin layers of Dinophysis acuminata *and other dinoflagellates*—Previous observations (Blanco et al. 1998; Tilstone et al. 2000) have supported the view that strong upwelling pulses in the Galician Rías Baixas disperse dinoflagellate populations offshore. However, this study shows that substantial numbers ($>10^3$ cell L^{-1}) of *D. acuminata* persisted in Ría de Pontevedra throughout an upwelling–downwelling cycle. This species, which in 2005 produced closures of mussel harvesting in the area in early March (INTECMAR, www.intecmar.org), exhibited a patchy distribution during the first 12 d of the cruise. Thus, *Dinophysis* spp. were not dispersed but aggregated in near-surface patches that were located in the top 6 m and associated with the diurnal thermocline. During relaxation, and in association with downwelling pulses, *Dinophysis* spp. appeared in high numbers ($>2 \times 10^3$ cell L^{-1}) and spread throughout the ría.

A common assumption is that dinoflagellates in general (Gentien at al. 2005) and *Dinophysis* spp. in particular (Maestrini 1998, and references therein), grow better in stratified environments. Further, Moita and Sampayo (1993) described putative cysts in a population of *Dinophysis caudata* and *Dinophysis tripos* in a convergence area. These authors suggested that cysts had been formed as a response to the stress caused by the downward flow of the water in the convergence area. The occurrence of high numbers of *Dinophysis* spp. in the Galician Rías has been associated with two different scenarios: in situ growth favored by periods of stratification between moderate upwelling pulses, and downwelling events that promote accumulation of large dinoflagellates, including *Dinophysis* spp., particularly at the end of the upwelling season (Reguera et al. 1995).

In our cruise, estimates of the intrinsic division rate (μ) of *D. acuminata* by the mitotic index approach (Reguera et al. 2003) during upwelling (03 June) and relaxation (09 June) showed moderate values of μ ($\mu_{min} \approx 0.16\ d^{-1}$),

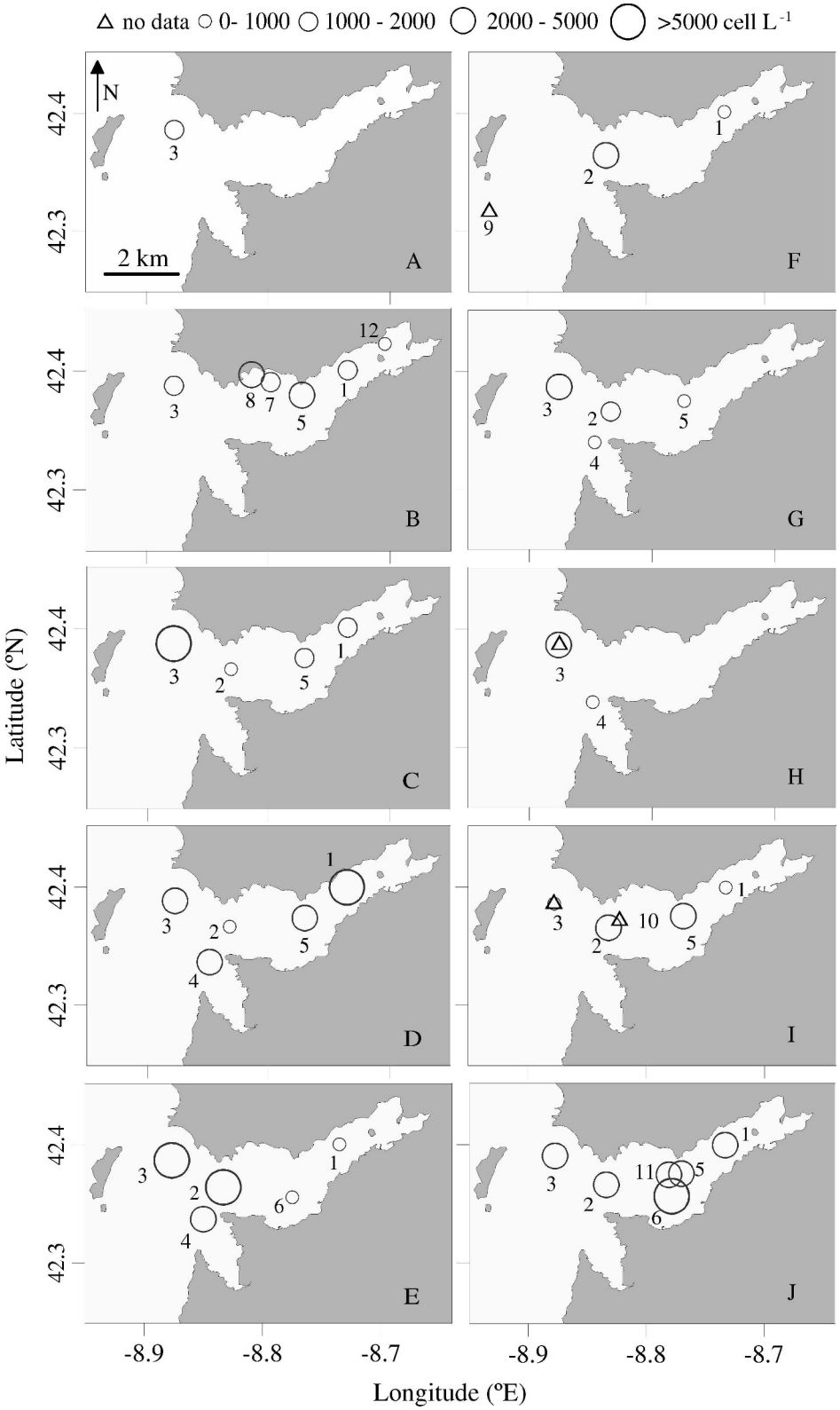

Fig. 15. Horizontal distribution of *D. acuminata* cell maxima in Ría of Pontevedra during the survey. (A) 31 May, (B) 01 June, (C) 02 June, (D) 03 June, (E) 06 June, (F) 07 June, (G) 08 June, (H) 09 June, (I) 10 June, and (J) 13 June. All dates are 2005.

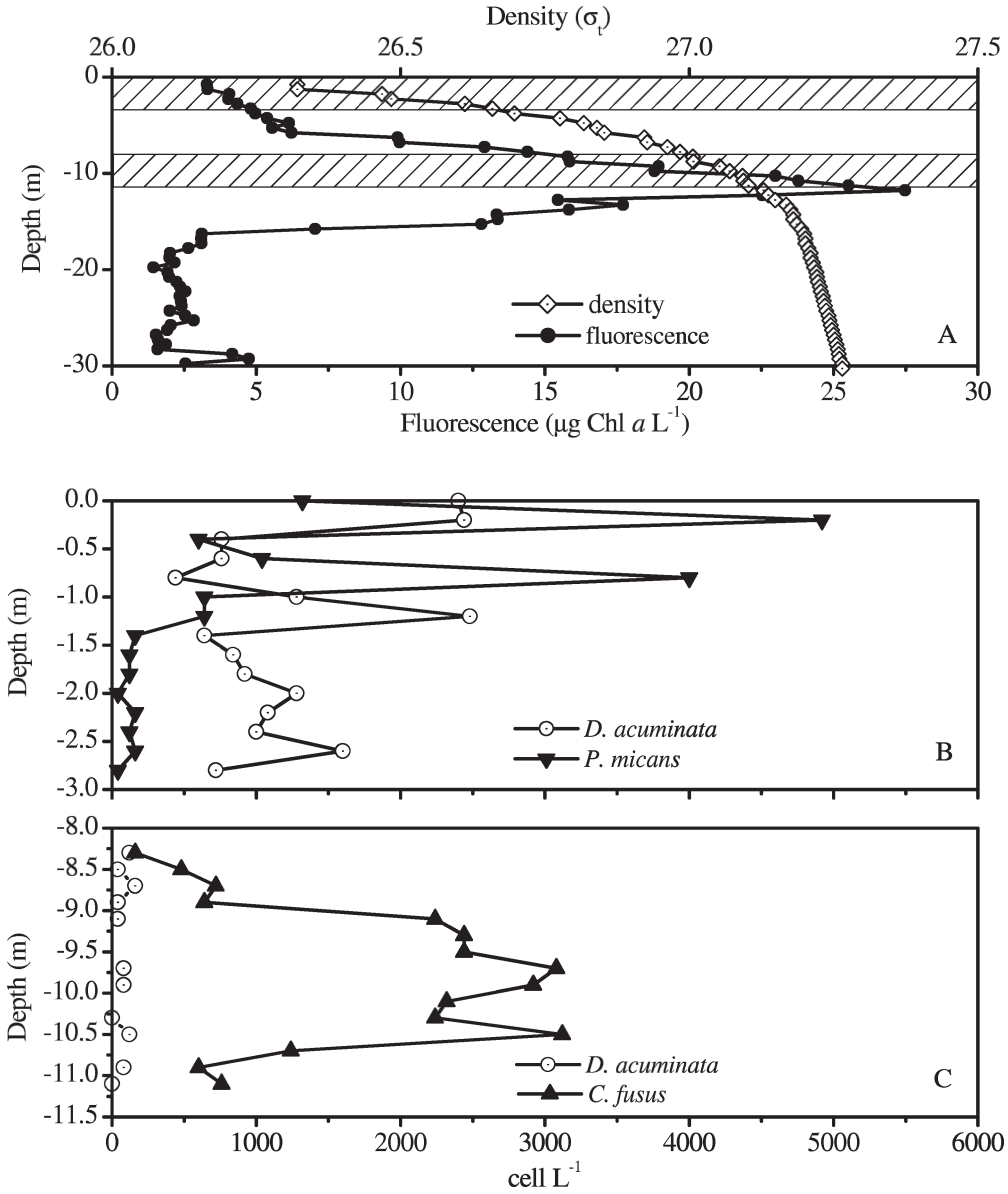

Fig. 16. (A) Vertical distribution of seawater density (σ_t) and in vivo fluorescence (μg Chl *a* L^{-1}) on 09 June at sta. 3. Depth ranges where the Fine-Scale Sampler (FSS) was deployed are shaded. (B) Vertical microdistribution (0–3 m) of *D. acuminata* and *P. micans* (cell L^{-1}). (C) Vertical microdistribution (8–11 m) of *D. acuminata* and *C. fusus* (cell L^{-1}).

whereas those during downwelling conditions (13–14 June) were much higher (μ_{min}= 0.25 d^{-1}, μ_{max}= 0.56 d^{-1}) (González-Gil et al. unpubl.). Therefore, downwelling pulses, at least those of the magnitude measured during this cruise, did not seem to inhibit *D. acuminata* division. The observed numerical increase would have resulted from both in situ division and physically driven accumulation, which selects for motile dinoflagellates under downwelling conditions (Fraga et al. 1988). Aggregation around a density gradient, with or without significant in situ division, may produce the frequent observations of *Dinophysis* maxima in stratified waters. A recent 24-h study of an autumn bloom of *D. acuta* in Ría de Pontevedra (Pizarro et al. 2008) showed that even in the case of a decaying population, with a division rate of almost zero, *Dinophysis* cells aggregated in a maximum around a shallow halocline.

The presence of *D. acuminata* at 21-m depth in the northern mouth of the ría on 31 May (sta. 3) deserves special attention. Given that high cell abundances of *D. acuminata* were always recorded at the surface after this date, this deeper-water *D. acuminata* population, transported into the rías by inflowing water may have acted as an inoculum and migrated from the upwelled waters into warmer subsurface waters to rebuild the preexisting population. A similar mechanism could explain the presence of the only *D. acuminata* cell maximum observed within the Chl *a* maximum at sta. 2 during the second upwelling pulse on 07 June. In a 10-yr time series study in the same ría, Pazos et al. (unpubl.) established a relation

between late initiation of *D. acuminata* populations and the lack of spring upwelling events. A similar mechanism was described by Townsend et al. (2001) for the transport of *Alexandrium* spp. cells by the Eastern Maine Coastal Current from offshore waters into the Gulf of Maine. Thus, upwelling pulses can represent a pathway through which recurrent *D. acuminata* populations, which wax and wane over the upwelling season (March–October) in the Galician Rías Baixas, are entrained from the adjacent shelf.

Although *D. acuminata* was not observed to perform diel vertical migration (DVM) during the present survey, DVM of *D. acuminata*, from about 10 m at night to 5 m at midday, has been reported in the Galician Rías (Villarino et al. 1995; Reguera et al. 2003). Nevertheless, a seasonal trend in the vertical distribution of the population, from early growth starting in deeper water to late stages aggregating near the surface, has been described for *D. acuminata* in the Rías (Escalera et al. 2006). Variations in the vertical distribution of the cell maxima for mixotrophic *Dinophysis* spp. could be attributed to different feeding behavior during different phases of the population. It was surprising that during this study, *D. acuminata* cell maxima were located in the top 5 m, where inorganic nutrients were depleted, high light intensities could produce photosynthesis inhibition, and where wind-forced surface currents were strongest. A change in cell appearance was observed—a progression from small nonvacuolated cells to highly vacuolated, large cells (González-Gil et al. unpubl.), possibly related to feeding on patches of *M. rubra*, which were also found in the surface waters. It may therefore be heterotrophic feeding, and the distribution of its specific prey (*M. rubra*), that caused *D. acuminata* to be located in the upper layers at this phase of the population growth.

High-resolution vertical distribution of Dinophysis *spp.*—*Dinophysis acuminata* and *P. micans* have often been cited as companion species (Kat 1979; Peperzak et al. 1996, and references therein). In fact, the dominance of *P. micans* coinciding with *D. acuminata* blooms and subsequent diarrhetic shellfish poisoning (DSP) events in Dutch coastal waters led to the historic misidentification of *P. micans* as the causative agent of these toxic outbreaks in the 1970s (Kat 1979). Samples collected with the FSS sampler show that both dinoflagellate species were in the surface layer, but their cell maxima were physically separated (at 0.2 m and 1.5 m, respectively). Thus, vertical fine scale sampling, at least in this particular case at this profile, showed a decimeter-scale segregation of *P. micans* and *D. acuminata* in the water column, where each species occupied a different niche within the vertical gradients of light and nutrients.

Implications for monitoring of potentially toxic phytoplankton and shellfish uptake of toxins—During this survey, sampling of the water column with a high-resolution profiler allowed the detection of high concentrations of phytoplankton in the pycnocline, 2–3 times higher than maximum values ever reported in the rías with conventional sampling methods (Nogueira et al. 1997). It also allowed us to track patches of *D. acuminata* near the surface that easily escaped monitoring observations.

The establishment of steep pycnoclines after upwelling pulses and the formation of TLs of *Pseudo-nitzschia* spp. and other diatoms suggest that pycnoclines may act as retention areas for these populations. *Pseudo-nitzschia* spp. have been reported before to form TLs associated with density gradients. Sullivan et al. (2005) described TLs of *Pseudo-nitzschia* spp. in Monterey Bay (California, U.S.A.) that persisted in the pycnocline for over one week. In the same area, Ryan et al. (2005) showed a subsurface layer of *Pseudo-nitzschia* spp. that had significantly variable thickness and boundaries along the sampled stations but that closely followed the pycnocline distribution in the bay. Rines et al. (2002) also described the development and posterior displacement of TLs of *Pseudo-nitzschia* spp. associated with density gradients in San Juan Islands (Washington, U.S.A.). In this study, they also observed two different TLs of *Pseudo-nitzschia* spp. in the water column, both associated with water masses characterized by different density signatures.

Results from different experiments with cultures have shown a higher toxin content per cell in the stationary phase of *Pseudo-nitzschia* spp. (Bates 1998). During the present survey, the observation of empty thecae and broken cells of *Pseudo-nitzschia* spp., which were present in the ría from early April (INTECMAR, www.intecmar.org), suggests that we were dealing with a decaying population, possibly with a high cellular content of domoic acid. The rapid descent of this "toxic mat" of *Pseudo-nitzschia* spp. following downwelling would explain a quite common event in the Galician Rías: the detection of domoic acid above regulatory levels in benthic shellfish resources earlier than in raft mussels, and its persistence in these wild shellfish banks long after it disappearance in mussels (Arévalo et al. 2001). Since downwelling of surface waters is a common feature in the Galician Rías Baixas during the upwelling season (March to October), dense bottom layers of toxic *Pseudo-nitzschia* populations represent a recurrent but predictable phenomenon associated with seasonal upwelling–downwelling cycles. In fact, shellfish harvesting in different areas of Ría de Pontevedra was prohibited during the two weeks of the cruise due the occurrence of both ASP and DSP toxins in shellfish above regulatory levels. At the end of the cruise, ASP toxins were virtually undetectable in mussels held on raft lines, but they were still found in benthic resources.

In waters off Seattle, Washington State (U.S.A. coast), Trainer et al. (2002) observed that transport of *Pseudo-nitzschia* spp. in the Juan de Fuca Eddy to the coast was associated with a quick rise of domoic acid content in shellfish above regulatory levels. These authors proposed that *Pseudo-nitzschia* spp. populations in nearshore waters generally did not reach high cell-toxin quotas and therefore did not lead to shellfish contamination with domoic acid. In contrast, populations from the Juan de Fuca Eddy, which acted as a retention area or incubator, matured and reached high cell-toxin quotas. In a similar way, the downwelling event could have pushed mature populations of *Pseudo-nitzschia* with high cell-toxin quota down to the seabed of the ría.

Subsurface TLs of *Pseudo-nitzschia* may be inadequately sampled or even missed by routine monitoring programs that

rely either on integrated water-column samples collected by hoses, or on oceanographic-bottle samples taken at specific depth intervals. Tracking near- surface *Dinophysis* patches can be an even more uncertain task. Routine weekly sampling by the Galician monitoring center showed very low cell numbers (120 cell L^{-1}) or even below detection levels of *D. acuminata* until 13 June, despite continuous detection of concentrations above 10^3 cell L^{-1} during the cruise. Therefore, hose-samplers, while effective for detection of harmful algae species throughout the water column, are not reliable for detection of TLs of toxic microalgae and may partly explain frequent bad correlations observed between cell numbers and toxin content in shellfish.

References

Álvarez, I., M. De Castro, R. Prego, and M. Gómez-Gesteira. 2003. Hydrographic characterization of a winter-upwelling event in the Ría of Pontevedra (NW Spain). Estuar. Coast. Shelf Sci. **56:** 869–876.

Álvarez-salgado, X. A., G. Rosón, F. F. Pérez, F. G. Figueiras, and Y. Pazos. 1993. Hydrographic variability off the Rías Baixas NW, Spain during the upwelling season. J. Geophys. Res. **98:** 14447–14455.

Aminot, A., and R. Kerouel. 2004. Hydrologie des écosystèmes marins. Paramètres et analyses. IFREMER.

Arévalo, F., C. Salgado, M. Bermúdez, and J. Correa. 2001. Control de biotoxinas en las áreas de producción de moluscos en Galicia. Seguimiento durante los años 1999–2000, p. 107–121. *In* VII Reunión Ibérica de Fitoplancton y Biotoxinas. Generalitat Valenciana, Alicante.

Bates, S. S. 1998. Ecophysiology and metabolism of ASP toxin production, p. 405–426. *In* D. M. Anderson, A. D. Cembella and G. M. Hallegraeff [eds.], Physiological ecology of harmful algal blooms. Springer-Verlag.

———, and V. Trainer. 2006. The ecology of harmful diatoms, p. 81–93. *In* E. Granéli and J. Turner [eds.], Ecology of harmful algae. Springer-Verlag.

Bendschneider, K., and R. J. Robinson. 1952. A new spectrophotometric method for the determination of nitrite in sea water. J. Mar. Res. **11:** 87–96.

Blanco, J., A. Moroño, Y. Pazos, J. Maneiro, and J. Mariño. 1998. Trends and variations of the abundance of main PSP and DSP producing species in the Galician Rías: Environmental and biological influences, p. 204–207. *In* B. Reguera, J. Blanco, M. L. Fénandez and T. Wyatt [eds.], Harmful algae. Xunta de Galicia and Intergovernmental Oceanographic Commission of UNESCO.

Boyle, J. A., J. D. Pickett-Heaps, and D. B. Czarnecki. 1984. Valve morphogenesis in the pennate diatom *Achnanthes coarctica*. J. Phycol. **20:** 563–573.

Carpenter, J. E., S. Janson, R. Boje, F. Pollehne, and J. Chang. 1995. The dinoflagellate *Dinophysis norvegica*: Biological and ecological observations in the Baltic Sea. Eur. J. Phycol. **30:** 1–9.

De Castro, M., M. Gómez-Gesteira, R. Prego, J. J. Taboada, P. Montero, P. Herbello, and V. Pérez-Villar. 2000. Wind and tidal influence on water circulation in a Galician Ría (NW Spain). Estuar. Coast. Shelf Sci. **51:** 161–176.

Dekshenieks, M. M., P. L. Donaghay, J. M. Sullivan, J. E. B. Rines, T. R. Osborn, and M. S. Twardowski. 2001. Temporal and spatial occurrence of thin phytoplankton layers in relation to physical processes. Mar. Ecol. Prog. Ser. **223:** 61–71.

Donaghay, P. L., and T. R. Osborn. 1997. Toward a theory of biological–physical control of harmful algal blooms dynamics and impacts. Limnol. Oceanogr. **42:** 1283–1296.

Escalera, L., B. Reguera, Y. Pazos, A. Moroño, and J. M. Cabanas. 2006. Are different species of *Dinophysis* selected by climatological conditions? Afr. J. Mar. Sci. **28:** 283–288.

Fiuza, A., M. Hamman, I. Ambar, G. Díaz del río, N. González, and J. M. Cabanas. 1998. Water masses and their circulation off western Iberia during May 2003. Deep-Sea Res. I **45:** 1127–1160.

Fraga, S., D. M. Anderson, I. Bravo, B. Reguera, K. A. Steidinger, and C. M. Yentsch. 1988. Influence of upwelling relaxation on dinoflagellates and shellfish toxicity in Ría de Vigo, Spain. Estuar. Coast. Shelf Sci. **27:** 349–361.

Fryxell, G., M. Villac, and L. P. Shapiro. 1997. The occurrence of the toxic diatom genus *Pseudo-nitzschia* (Bacillariophyceae) on the West Coast of USA, 1920–1996: A review. Phycologia **36:** 419–437.

Gallager, S. M., H. Yamazaki, and C. S. Davis. 2004. Contribution of fine-scale vertical structure and swimming behavior to formation of plankton layers on Georges Bank. Mar. Ecol. Prog. Ser. **267:** 27–43.

Genin, A., J. S. Jaffe, R. Reef, C. Richter, and P. J. S. Franks. 2005. Swimming against the flow: A mechanism of zooplankton aggregation. Science **308:** 860–862.

Gentien, P., P. L. Donaghay, H. Yamazaki, R. Raine, B. Reguera, and T. R. Osborn. 2005. Harmful algal blooms in stratified environments. Oceanography **18:** 172–183.

———, M. Lunven, M. Lehaître, and J. L. Duvent. 1995. In situ depth profiling of particles sizes. Deep-Sea Res. I **42:** 1297–1312.

Grasshoff, K., M. Ehrhardt and K. Kremling [eds.]. 1983. Methods of seawater analysis. 2nd ed. Verlag Chemie.

Holliday, D. V., P. L. Donaghay, C. F. Greenlaw, D. E. McGehee, M. M. McManus, J. M. Sullivan, and J. L. Miksis. 2003. Advances in defining fine- and micro- scale pattern in marine plankton. Aquat. Liv. Res. **16:** 131–136.

INTECMAR. [Accessed 15 June 2005] <http://www.intecmar.org>.

Kat, M. 1979. The occurrence of *Prorocentrum* species and coincidental gastroenteritis illness of mussel consumers, p. 215–220. *In* D. L. Taylor and H. H. Seliger [eds.], Toxic dinoflagellate blooms. Elsevier.

Klausmeier, C. A., and E. Litchman. 2001. Algal games: The vertical distribution of phytoplankton in poorly mixed waters. Limnol. Oceanogr. **46:** 1998–2007.

Kononen, K., M. Huttunen, S. Hallfors, P. Gentien, M. Lunven, T. T. Huttula, J. Laanemets, M. Lilover, J. Pavelson, and A. Stips. 2003. Development of a deep chlorophyll maximum of *Heterocapsa triquetra* Ehrenb. at the entrance to the Gulf of Finland. Limnol. Oceanogr. **48:** 594–607.

Koukaras, K., and G. Nikolaidis. 2004. *Dinophysis* blooms in Greek coastal waters (Thermaikos Gulf, NW Aegean Sea). J. Plankton Res. **26:** 445–457.

Lindahl, O., B. Lundve, and M. Johansen. 2007. Toxicity of *Dinophysis* spp. in relation to population density and environmental conditions on the Swedish west coast. Harmful Algae **6:** 218–231.

Lunven, M., P. Gentien, K. Kononen, E. Le Gall, and M. M. Danielou. 2003. In situ video and diffraction analysis of marine particles. Estuar. Coast. Shelf Sci. **57:** 1127–1137.

———, J. F. Guillaud, A. Youenou, M. P. Crassous, R. Berric, E. Le Gall, R. Kerouel, C. Labry, and A. Aminot. 2005. Nutrient and phytoplankton distribution in the Loire River plume (Bay of Biscay, France) resolved by a new Fine Scale Sampler. Estuar. Coast. Shelf Sci. **65:** 94–108.

Maestrini, S. Y. 1998. Bloom dynamics and ecophysiology of *Dinophysis* spp., p. 243–266. *In* D. M. Anderson, A. D. Cembella and G. M. Hallegraeff [eds.], Physiological ecology of harmful algal blooms. NATO ASI Series G, Ecological Sciences 41. Springer-Verlag.

McManus, M. A., O. M. Cherinton, P. J. Drake, D. V. Holliday, C. D. Storlazzi, P. L. Donaghay, and C. F. Greenlaw. 2005. Effects of physical processes on structure and transport of thin zooplankton layers in the coastal ocean. Mar. Ecol. Prog. Ser. **301:** 199–215.

———, and others. 2003. Characteristics, distribution and persistence of thin layers over a 48 hour period. Mar. Ecol. Prog. Ser. **261:** 1–19.

Míguez, A., M. L. Fernández, and S. Fraga. 1996. First detection of domoic acid in Galicia (NW of Spain), p. 143–145. *In* T. Yasumoto, Y. Oshima and Y. Fukuyo [eds.], Harmful and toxic algal blooms. Intergovernmental Oceanographic Commission of UNESCO.

Moita, M. T., and M. A. Sampayo. 1993. Are there cysts in the genus *Dinophysis*? p. 153–157. *In* T. Smayda and Y. Shimizu [eds.], Toxic phytoplankton blooms in the sea. Elsevier.

———, L. Sobrinho-Gonçalves, P. B. Oliveira, S. Palma, and M. Falcão. 2006. A bloom of *Dinophysis acuta* in a thin layer off North-West Portugal. Afr. J. Mar. Sci. **28:** 265–269.

Nogueira, E., F. F. Pérez, and A. F. Ríos. 1997. Seasonal patterns and long-term trends in an estuarine upwelling ecosystem (Ría de Vigo, NW Spain). Estuar. Coast. Shelf Sci. **44:** 285–300.

Park, M. G., K. Sunju, H. S. Kim, G. Myung, Y. G. Kang, and W. Yih. 2006. First successful culture of the marine dinoflagellate *Dinophysis acuminata*. Aquat. Microb. Ecol. **45:** 101–106.

Peperzak, L. G., J. Snoeijer, R. Dijkema, W. W. C. Gieskes, J. Joordens, J. C. H. Peeters, C. Schol, E. G. Vrieling, and W. Zevenboom. 1996. Development of *Dinophysis acuminata* bloom in the river Rhine plume (North Sea), p. 273–276. *In* T. Yasumoto, Y. Oshima and Y. Fukuyo [eds.], Harmful and toxic algal blooms. Intergovernmental Oceanographic Commission of UNESCO.

Pizarro, G., L. Escalera, S. González-Gil, J. M. Franco, and B. Reguera. 2008. Growth, behaviour and cell toxin quota of *Dinophysis acuta* during a daily cycle. Mar. Ecol. Prog. Ser. **353:** 89–105.

Prego, R., A. W. Dale, M. De Castro, M. Gómez-Gesteira, J. J. Taboada, P. Montero, M. Ruiz-Villareal, and V. Pérez-Villar. 2001. Hydrography of the Pontevedra Ría: Intra-annual spatial and temporal variability in a Galician coastal system (NW Spain). J. Geophys. Res. **106:** 19845–19857.

Reguera, B., I. Bravo, and S. Fraga. 1995. Autoecology and some life history stages of *Dinophysis acuta* Ehrenberg. J. Plankton Res. **17:** 999–1015.

———, E. Garcés, I. Bravo, Y. Pazos, I. Ramilo, and S. González-Gil. 2003. Cell cycle patterns and estimates of in situ division rates of dinoflagellates of the genus *Dinophysis* by a postmitotic index. Mar. Ecol. Prog. Ser. **249:** 117–131.

Rines, J. E. B., P. L. Donaghay, M. M. Dekshenieks, J. M. Sullivan, and M. S. Twardowski. 2002. Thin layers and camouflage: Hidden *Pseudo-nitzschia* spp. (Bacillariophyceae) populations in a fjord in the San Juan Islands, Washington, USA. Mar. Ecol. Prog. Ser. **225:** 123–137.

Ryan, J. P., F. P. Chavez, and J. G. Bellingham. 2005. Physical–biological coupling in Monterey Bay, California: Topographic influences on phytoplankton ecology. Mar. Ecol. Prog. Ser. **287:** 23–32.

Setälä, O., R. Autio, H. Kuosac, J. Rintala, and P. Ylostalob. 2005. Survival and photosynthetic activity of different *Dinophysis acuminata* populations in the northern Baltic Sea. Harmful Algae **4:** 337–350.

Sharples, J., C. M. Moore, T. P. Rippeth, P. M. Holligan, D. J. Hydes, N. R. Fisher, and J. H. Simpson. 2001. Phytoplankton distribution and survival in the thermocline. Limnol. Oceanogr. **46:** 486–496.

Stacey, M. T., M. A. McManus, and J. V. Steinbuck. 2007. Convergences and divergences and thin layer formation and maintenance. Limnol. Oceanogr. **52:** 1523–1532.

Sullivan, J. M., M. S. Twardowsli, P. L. Donaghay, and S. A. Freeman. 2005. Use of optical scattering to discriminate particle types in coastal waters. Appl. Optics **44:** 1667–1680.

Tilstone, G. H., B. M. Míguez, F. G. Figueiras, and E. G. Fermín. 2000. Diatom dynamics in a coastal ecosystem affected by upwelling: Coupling between species succession, circulation and biogeochemical processes. Mar. Ecol. Prog. Ser. **205:** 23–41.

Townsend, D. W., N. R. Pettigrew, and A. C. Thomas. 2001. Offshore blooms of the red tide dinoflagellate, *Alexandrium* spp., in the Gulf of Maine. Cont. Shelf Res. **21:** 347–369.

Trainer, V. L., B. M. Hickey, and R. Homer. 2002. Biological and physical dynamics of domoic acid production off the Washington coast. Limnol. Oceanogr. **47:** 1438–1446.

Utermöhl, H. 1931. Neue wege in der quantitativen Erfassung des Planktons (mit besonderer Berücksichtigung des Ultraplanktons). Verh. Int. Ver. Theor. Angew. Limnol. **5:** 567–596.

Villarino, M. L., F. G. Figueiras, K. J. Jones, X. A. Álvarez-Salgado, J. Richard, and A. Edwards. 1995. Evidence of in situ diel vertical migration of a red-tide microplankton species in Ría de Vigo (NW Spain). Mar. Biol. **123:** 607–617.

Wood, E., F. A. J. Armstrong, and F. A. Richards. 1967. Determination of nitrate in sea water by cadmium-copper reduction to nitrite. J. Mar. Biol. Assoc. UK **47:** 23–31.

Received: 30 July 2007
Accepted: 18 January 2008
Amended: 19 February 2008